



## Characterization and catalytic performance of Co/SBA-15 supported gold catalysts for CO oxidation

Xiuyan Xu, Jinjun Li, Zhengping Hao<sup>\*</sup>, Wei Zhao, Chun Hu

*Research Center for Eco-Environmental Sciences, Chinese Academy of Sciences, Beijing 100085, China*

Received 6 April 2005; received in revised form 19 July 2005; accepted 2 August 2005

Available online 24 August 2005

---

### Abstract

Cobalt-containing SBA-15 supported gold catalysts for low-temperature CO oxidation were prepared and characterized by N<sub>2</sub> adsorption/desorption, X-ray diffraction, transmission electron microscopy, inductively coupled plasma-atom emission spectroscopy and X-ray photoelectron spectroscopy techniques. The effects of cobalt and gold content on the catalyst activity were investigated in detail. Among them, 2% Au/40% Co/SBA-15 shows the highest activity, its complete conversion temperature for CO is at 273 K. It was believed that both the dispersion of Co<sub>3</sub>O<sub>4</sub> and the high surface areas caused by SBA-15 contribute to the good activities of cobalt-containing SBA-15 supported gold catalysts. Furthermore, the strong metal-support interaction between gold and cobalt oxides is greatly related to the catalytic performance.

© 2005 Elsevier Ltd. All rights reserved.

*Keywords:* A. Metals; C. X-ray diffraction; A. Oxides

---

### 1. Introduction

The interest in studying on nano-gold catalyst has increased substantially since Haruta et al. discovered the special activity of supported gold catalyst for low temperature CO oxidation [1]. Lots of the studies have been carried out in this field [2–5]. Generally, the catalytic activity of gold catalyst critically depends on the support material, the preparation methods, and the activation procedure. The explanations for the catalytic activity have mainly focused on the size of the gold particles and the nature

---

<sup>\*</sup> Corresponding author. Tel.: +86 10 62849194; fax: +86 10 62923564.

*E-mail address:* [zpinghao@mail.rcees.ac.cn](mailto:zpinghao@mail.rcees.ac.cn) (Z. Hao).

of the support. For an active gold catalyst, small gold particles with size of less than 5 nm are necessary, and the gold nanoparticles are usually supported on metal oxide supports. Gold catalysts supported on a single metal oxide have been extensively studied [6–8], and SiO<sub>2</sub> has been regarded as an inactive support because of the weak interaction between the gold and the support [9,10]. However, gold catalysts supported on reducible transition oxides exhibit very high activities [6].

Recently, the use of periodic mesoporous silicas as supports for preparing Co-based catalysts for Fischer–Tropsch synthesis has been explored [11,12]. The very high surface areas characteristic of mesoporous molecular sieves make it possible for higher cobalt loading and higher dispersions as compared with conventional amorphous silica. Moreover, the presence of a uniform pore-size distribution in the ordered mesoporous materials should allow, in principle, for a better control on the cobalt particle size and the catalytic properties. Therefore, it seems possible to prepare an active gold catalyst using cobalt-containing periodic mesoporous silica as support. SBA-15 is a type of mesoporous silica, which possesses a high surface area (600–1000 m<sup>2</sup>/g) and a hexagonal array of uniform tubular channels with pore diameters ranging from 5 to 30 nm [13].

In the present work, cobalt-containing SBA-15 supported gold catalysts for low-temperature CO oxidation were prepared and characterized by N<sub>2</sub> adsorption/desorption, XRD, TEM, ICP-AES and XPS techniques. The effects of cobalt and gold content on the catalyst activity were investigated in detail, and the relationship between structural changes and activity data was discussed.

## 2. Experimental

A pure SBA-15 sample was synthesized by a similar method as described in the literature [14]. The samples of Co/SBA-15 were prepared by incipient-wetness impregnation with cobalt nitrate solution. The impregnated samples were dried at 373 K overnight, followed by calcinations at 773 K for 3 h. Co/SBA-15 supported gold catalysts were prepared by deposition–precipitation with urea as a precipitation agent [15]. In a typical synthesis, 1.5 g of Co/SBA-15 was added to 100 ml of an aqueous solution containing HAuCl<sub>4</sub> and urea, the initial pH was about 2. The suspension was vigorously stirred at 353 K for 4 h. Urea decomposition led to a gradual rise of pH from 2 to 7. Then the solids were centrifuged and washed by hot deionized water until they were free of chloride ions. Finally the solids were dried at 343 K, and calcined at 573 K for 3 h with a heating rate of 5 K/min. The final catalysts were named as  $\omega_1$  Au/ $\omega_2$  Co/SBA-15, where  $\omega_1$  and  $\omega_2$  denote the weight percent of gold atom and cobalt atom in the sample, respectively.

The textural properties of the samples were measured by nitrogen adsorption/desorption at liquid nitrogen temperature, using a gas adsorption analyzer NOVA 1200. The gold content of the catalysts was analyzed with inductively coupled plasma-atom emission spectroscopy (ICP-AES) using a ULTIMA spectrometer. X-ray photoelectron spectroscopy (XPS) data were accumulated on an Axis Ultra ESCA system with a monochromatic Al K $\alpha$  standard radiation source. The binding energies were calibrated by referencing the C 1s at 284.8 eV. XRD analysis was performed on a D5005D X-ray diffractometer. Diffraction patterns were recorded with Cu K $\alpha$  radiation (40 mA, 40 kV). Transmission electron microscopy (TEM) measurements were carried out on a H-800 microscope operating at 200 kV. Prior to the experiment, the samples were dispersed in ethanol by sonication and dropped on a copper grid coated with a carbon film.

The catalytic activity was investigated in a fixed bed reactor, and the temperature of catalyst bed was measured by a thermocouple. A sample (100 mg, 60–80 mesh) was placed in a quartz tube with an inner

diameter of 6 mm. A mixture of CO and air (5047 ppm CO, balance air) was admitted at a flow rate of 66.7 ml/min, resulting in a space velocity of  $40\,000\text{ ml h}^{-1}\text{ g}_{\text{cat}}^{-1}$ . The exit gases from the catalyst reactor were analyzed by an on-line gas chromatography (SP-2100), equipped with a hydrogen flame ionization detector connected with a carbon sieve column.

### 3. Results and discussion

The nitrogen adsorption–desorption isotherms for SBA-15 and various cobalt-containing samples were shown in Fig. 1. The isotherm (Fig. 1a) exhibits a hysteresis loop, which is typical for capillary condensation of nitrogen in the mesopores. The mesoporous regularity is confirmed by a narrow interval of relative pressure  $\Delta(P/P_0) = 0.2$ . The shape of the  $\text{N}_2$  adsorption–desorption isotherm of cobalt-containing SBA-15 is similar to that of the pure SBA-15, indicating that the mesoporous structure of SBA-15 is mostly maintained upon cobalt oxide impregnation.

Compared with the pure SBA-15, the inflection of the adsorption branch of the isotherm (Fig. 1b and c) occurred at a lower relative pressure for cobalt-containing samples, indicating a decrease of the pore diameter after cobalt incorporation. The textural properties of all the samples were listed in Table 1. Upon impregnation of SBA-15 with cobalt oxides, a substantial loss in the BET surface area and the total pore volume could be observed. The decrease is mainly caused by the partial blockage of the SBA-15 pores. However, after deposition of a small amount of gold particles on cobalt-containing SBA-15, apart from a certain loss happened in the pore volume, a substantial widening in pore-size and an obvious decrease in the surface area were observed, which could be resulted from the partial degradation of silica matrix in basic media caused by urea hydrolysis during gold deposition.

Typical TEM micrograph of the pure SBA-15 (Fig. 2a) shows the highly ordered arrangement of the pore channels. The TEM micrograph of 40% Co/SBA-15 reveals that some cobalt oxides are located

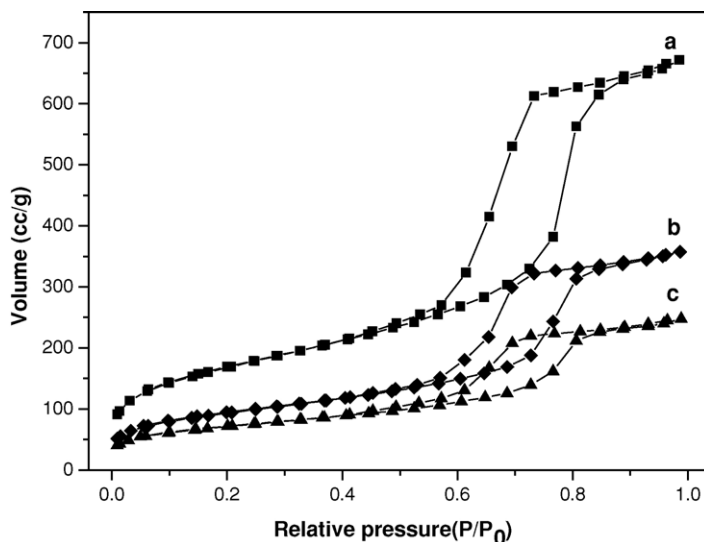


Fig. 1. Nitrogen adsorption/desorption isotherm for: (a) SBA-15; (b) 28% Co/SBA-15; (c) 40% Co/SBA-15.

Table 1  
Textural property of supports and catalysts

Sample	$S_{\text{BET}}^{\text{a}}$ ( $\text{m}^2/\text{g}$ )	$V_{\text{p}}^{\text{b}}$ ( $\text{cm}^3/\text{g}$ )	$D_{\text{p}}^{\text{c}}$ (nm)
SBA-15	604	1.03	6.8
28% Co/SBA-15	336	0.55	6.5
40% Co/SBA-15	254	0.38	6.0
2% Au/28% Co/SBA-15	240	0.49	7.7
4% Au/28% Co/SBA-15	231	0.46	7.9
1% Au/40% Co/SBA-15	167	0.37	7.6
2% Au/40% Co/SBA-15	172	0.36	8.4

<sup>a</sup> BET specific surface areas.

<sup>b</sup> Total pore volumes are obtained at  $P/P_0 = 0.99$ .

<sup>c</sup> Average pore diameters.

inside of the pores, while others are present on the external surface (Fig. 2b). In the TEM image of the 2% Au/40% Co/SBA-15 sample (Fig. 2c), gold particles (indicated by arrows) are clearly visible as spherical dark particles being different from cobalt oxides. All the observed gold particles are very small, and most of them are less than 5 nm.

The wide-angle XRD patterns for different Co-containing SBA-15 in comparison with the bulk  $\text{Co}_3\text{O}_4$  were shown in Fig. 3. All samples reveal the peak characteristic of  $\text{Co}_3\text{O}_4$  spinel at  $2\theta = 36.9^\circ$ . The peak becomes higher and narrower with increase of the cobalt oxides, indicating a gradual growth of the  $\text{Co}_3\text{O}_4$  crystallite size. According to Scherrer equation [16], crystallite size of pure  $\text{Co}_3\text{O}_4$  is calculated as 26.5 nm, while that of 28% Co/SBA-15 and 40% Co/SBA-15 are 11.0 and 15.4 nm, respectively. The results indicate that the SBA-15 frameworks have the high surface area and are favorable for the dispersion of  $\text{Co}_3\text{O}_4$ .

Fig. 4 presented the XRD patterns of different gold catalysts. Two percent Au/SBA-15 shows the peak characteristic of gold at  $2\theta = 38.2^\circ$ , and the peak is so sharp that the gold crystallite size calculated from Scherrer equation is as large as 19.3 nm, which is responsible for its poor catalytic activity. In contrast, there are no obvious XRD lines pertaining to crystallize gold in the case of 2% Au/40% Co/SBA-15, indicating that the deposited gold is highly dispersed on the surface of the 40% Co/SBA-15 support.

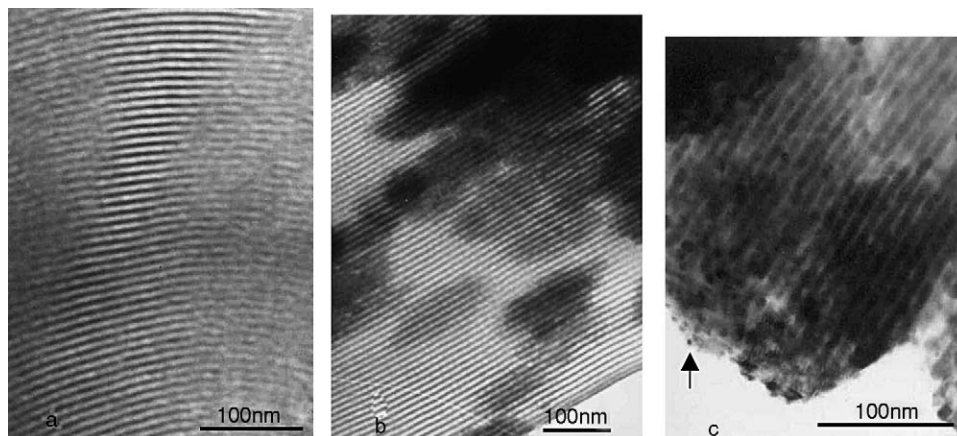


Fig. 2. TEM images of different samples: (a) SBA-15; (b) 40% Co/SBA-15; (c) 2% Au/40% Co/SBA-15.

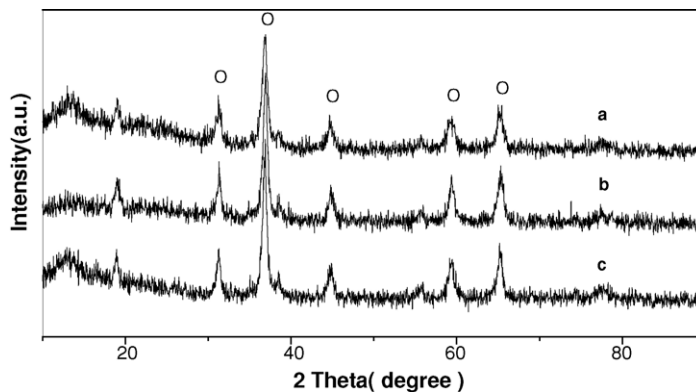


Fig. 3. X-ray diffraction patterns for Co-containing SBA-15 and bulk  $\text{Co}_3\text{O}_4$ : (a) 28% Co/SBA-15; (b) 40% Co/SBA-15; (c)  $\text{Co}_3\text{O}_4$  (○:  $\text{Co}_3\text{O}_4$ ).

In order to explore the gold content on the catalyst surface and that in the whole material, the related element composition was determined by XPS and ICP-AES, respectively. The gold content on the surface phase is 7.30%, which is far higher than that in the whole catalysts (1.65%), indicating that gold nanoparticles are mostly deposited on the surface of the 40% Co/SBA-15.

XPS spectra of the Au 4f and Co 2p binding energies of 2% Au/40% Co-SBA-15 were shown in Fig. 5. The peaks of Au  $4f_{5/2}$  and  $4f_{7/2}$  are centered at 87.5 and 83.8 eV, respectively, indicating the presence of gold in the metallic state [17]. These results are in good agreement with the literature results that gold is present just as  $\text{Au}^0$  at calcination temperature of higher than 573 K [18,19]. The Co 2p spectra shows the shake-up satellites with low intensity and a main peak at BE = 779.9 eV, which is typical for  $\text{Co}^{2+}/\text{Co}^{3+}$  ions in the  $\text{Co}_3\text{O}_4$  spinel phase [20]. Therefore,  $\text{Co}_3\text{O}_4$  is the predominant cobalt phase in the catalyst after calcination at 773 K.

The activities of Co/SBA-15 and various gold-containing catalysts were listed in Table 2. It was found that the pure SBA-15 is not active for CO oxidation, and 2% Au/SBA-15 has only 12% CO conversion even when the temperature is raised up to 573 K. Whereas, the introduction of cobalt oxide into SBA-15 could improve the catalytic activity, and the catalytic activities depend on the content of the cobalt to

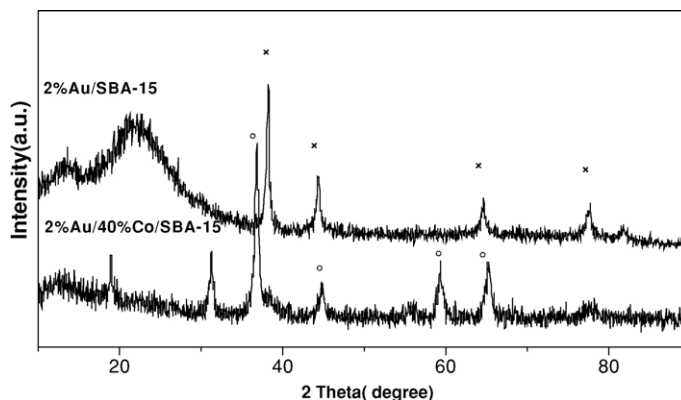


Fig. 4. X-ray diffraction patterns for different gold catalysts: (○)  $\text{Co}_3\text{O}_4$ ; (×) Au.

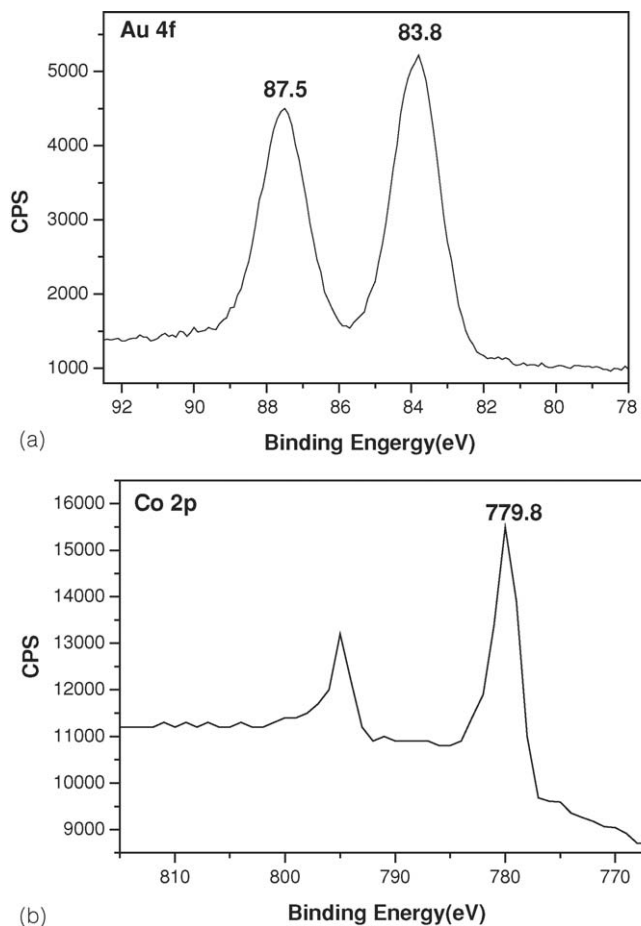


Fig. 5. X-ray photoelectron spectra of 2% Au/40% Co/SBA-15.

Table 2  
CO oxidation activities over different catalysts

Catalyst	CO conversion at 298 K (%)	$T_{100\%}$ (K)
SBA-15	0	>573
28% Co/SBA-15	0	463
40% Co/SBA-15	0	423
2% Au/SBA-15	0	>573
2% Au/28% Co/SBA-15	12	398
4% Au/28% Co/SBA-15	60	328
1% Au/40% Co/SBA-15	85	318
2% Au/40% Co/SBA-15	100	273
0.5% Au/40% Co/SBA-15	31	363
0.5% $\text{Co}_3\text{O}_4$	28	383

some extent. However, when the cobalt loading is up to 40%, it becomes difficult to impregnate more cobalt oxides into SBA-15. In the case of 40% Co/SBA-15, the complete oxidation temperature for CO has decreased to 423 K. Additionally, with the same cobalt-containing supports, the catalytic activity rises with increase of gold content. With the different cobalt-containing supports, however, it should be noticed that 4% Au/28% Co/SBA-15 shows poorer activity than 2% Au/40% Co/SBA-15, despite that 4% Au/28% Co/SBA-15 possesses higher gold content than 2% Au/40% Co/SBA-15. These could be assigned to the strong metal–support interaction (SMSI) between gold and cobalt oxides, which greatly related to the catalytic performance. There has been proposed that SMSI effects are caused by electron transfer between the support and metal or by intermetallic compounds of support and metal atoms [21]. Moreover, it should be noticed that 0.5% Au/40% Co/SBA-15 shows better activity than 0.5% Au/Co<sub>3</sub>O<sub>4</sub>, indicating that the cobalt oxides in the relatively high dispersion state caused by the channel system of SBA-15 are beneficial to the catalytic activity.

#### 4. Conclusion

Cobalt-containing SBA-15 materials are suitable supports for preparing active nano-gold catalysts for low-temperature CO oxidation. SBA-15 frameworks have the high surface areas and are favorable for the dispersion of Co<sub>3</sub>O<sub>4</sub>, which are responsible for CO oxidation activity. In addition, the strong interaction between cobalt oxides and gold on SBA-15 is also a key factor for the good activities of the gold catalysts.

#### Acknowledgements

This work was financially supported by the National Basic Research Program of China (2004CB719500), the key project of Knowledge Innovation of Chinese Academy of Sciences (KZCX3-SW-430) and the National Science Foundation of China (50278094, 20322201).

#### References

- [1] M. Haruta, N. Yamada, T. Kobayashi, S. Iijima, *J. Catal.* 115 (1989) 301.
- [2] G.R. Baumweda, S. Tsubota, T. Nakamura, M. Haruta, *Catal. Lett.* 44 (1997) 83.
- [3] H.H. Kung, M.C. Kung, C.K. Costello, *J. Catal.* 216 (2003) 425.
- [4] D.H. Wang, Z.P. Hao, D.Y. Cheng, X.C. Shi, C. Hu, *J. Mol. Catal. A* 200 (2003) 229.
- [5] D.A. Bulushev, I.Y. Elena, I. Suvorova, P.A. Buffat, L.K. Minsker, *J. Catal.* 224 (2004) 8.
- [6] M. Haruta, S. Tsubota, T. Kobayashi, H. Kageyama, M.J. Genet, B. Delmon, *J. Catal.* 144 (1993) 175.
- [7] A. Knell, P. Barnickel, A. Baiker, A. Wokaun, *J. Catal.* 137 (1992) 306.
- [8] C.K. Costello, M.C. Kung, H.-S. Oh, Y. Wang, H.H. Kung, *Appl. Catal. A* 232 (2002) 159.
- [9] A. Wolf, F. Schüth, *Appl. Catal. A* 226 (2002) 1.
- [10] A.M. Venezia, L.F. Liotta, G. Pantaleo, V. La Parola, G. Deganello, A. Beck, Zs. Koppány, K. Frey, D. Horváth, L. Guzzi, *Appl. Catal. A* 251 (2003) 359.
- [11] A. Martínez, C. López, F. Márquez, I. Díaz, *J. Catal.* 220 (2003) 486.
- [12] Y. Ohtsuka, Y. Takahashi, M. Noguchi, T. Arai, S. Takasaki, N. Tsubouchi, Y. Wang, *Catal. Today* 89 (2004) 419.
- [13] D. Zhao, J. Feng, Q. Huo, N. Melosh, G.H. Fredrickson, B.F. Chmelka, G.D. Stucky, *Science* 279 (1998) 548.
- [14] D. Zhao, Q. Huo, J. Feng, B.F. Chmelka, G.D. Stucky, *J. Am. Chem. Soc.* 120 (1998) 6024.

- [15] R. Zanella, S. Giorgio, C.R. Henry, C. Louis, *J. Phys. Chem. B* 106 (2002) 7634.
- [16] S. Villain, J. Cabané, P. Knauth, *Sci. Mater.* 38 (1998) 1003.
- [17] B. Koslowski, H.G. Boyen, C. Widerotter, G. Kastle, P. Ziemann, R. Wahrenberg, P. Oelhafen, *Surf. Sci.* 475 (2001) 1.
- [18] S. Minicò, S. Scirè, C. Crisafulli, S. Galvagno, *Appl. Catal. B* 34 (2001) 277.
- [19] E.D. Park, J.S. Lee, *J. Catal.* 186 (1999) 1.
- [20] Y. Brik, M. Kacimi, M. Ziyad, F. Bozon-Verduraz, *J. Catal.* 202 (2001) 118.
- [21] E.S. Shpiro, B.B. Dysenbina, O.P. Tkachenko, G.V. Antoshin, Kh.M. Minachev, *J. Catal.* 110 (1988) 262.